

Imaging and Measurement of Thermal Lensing in Glass and Sapphire Crystal

A thesis submitted in partial fulfillment of the requirement for the degree of
Bachelor of Science with Honors in Physics from
The College of William and Mary in Virginia,

by

Kyle Randall Wisian

Accepted for _____

Jan L. Chaloupka _____
Advisor

Robert M. Lewis _____

Henry Krakauer _____

Abstract

Now that physicists are using ultra-fast laser oscillators to research high-field atomic physics, amplification of short laser pulses is becoming more common. Because of the high energy needed to optically pump the lasing medium for pulse amplification, laser systems often suffer from thermal lensing. Corrective lenses may be installed in the system to counter the effects of the thermal lens, but different conditions require different corrective lenses.

It is the scope of this project to try to identify, understand, and measure thermal lensing in a few materials. Using a pump laser to induce thermal lensing in glass, we have been able to characterize the focal length of the lens as a function of absorbed pump power in glass, as well as to find some interesting ways of imaging the thermal lensing phenomenon.

Table of Contents

| | |
|--|----|
| Acknowledgement | 4 |
| 1.0 Introduction | 5 |
| 2.0 Background | 6 |
| 2.1 What is light? | 6 |
| 2.2 The Laser | 9 |
| 2.3 The Laser Oscillator | 12 |
| 2.4 Chirped Pulse Amplification | 15 |
| 3.0 Thermal Lensing | 18 |
| 4.0 Experiments and Results | 20 |
| 4.1 Interferometric Imaging of Thermal Lens in Glass | 20 |
| 4.1.1 Interferometric Imaging of Thermal Lens in Glass Results | 24 |
| 4.2 Focusing due to Thermal Lens in Glass | 26 |
| 4.2.1 Focusing due to Thermal Lens in Glass Results | 28 |
| 4.3 Focusing due to Thermal Lens in Sapphire | 30 |
| 4.3.1 Focusing due to Thermal Lens in Sapphire Results | 32 |
| 4.4 Mach-Zehnder Interferometric Imagery | 33 |
| 4.5 Combination Interferometric Imagery | 34 |
| 4.5.1 Combination Interferometric Imagery Results | 35 |
| 4.6 Intensity Measurement at Beam Center Using Pin Diode | 37 |
| 4.6.1 Intensity Measurement at Beam Center Using Pin Diode Results | 38 |
| 4.7 Effect of Cooling on Thermal Lensing in Glass | 38 |
| 5.0 Conclusions and Future Work | 39 |

| | |
|------------------------------|-----------|
| 5.1 Conclusions | 39 |
| 5.2 Future Work | 40 |
| References | 41 |

Acknowledgement

I would like to thank my advisor, Prof. Jan Chaloupka for putting so much time and effort into helping me with my research. He was faced with the daunting task of advising an optics project for someone with no optics training, as no true optics classes are offered at The College of William and Mary. He took the extra time to teach me things that weren't taught in the classroom. I would also like to thank Prof. Robert Lewis and Prof. Henry Krakauer for agreeing to serve on my committee and taking the time out of their busy schedules to be here and review my research. I would also like to thank Kirk Jacobs for his advice and help with the construction of the custom optics mounts used in the experiment.

1 Introduction

In strong-field atomic physics, researchers are now using ultra-fast lasers to probe intense laser-matter interactions. In the strong-field regime, the magnitude of the electric field associated with the laser pulse rivals the binding energy of an electron to an atom. The atomic unit of field strength occurs for an amplitude equivalent to that which binds the electron to the proton in a hydrogen atom. This occurs at an intensity of

$3.5 \times 10^{16} \frac{W}{cm^2}$ [7]. In order to effectively reach the strong-field regime, the modest

output from a laser oscillator must be amplified while maintaining the pulse's short duration. Two schemes, the regenerative and multi-pass amplifiers, are used to achieve the high pulse energies needed. Both of these solid state amplifiers rely on high energy pump lasers to optically pump the lasing medium for amplification of the ultra-short pulses. The intense energy from these pump lasers heats up the lasing medium and causing changes to its index of refraction. The index of refraction changes cause the lasing medium to act as a tiny thermal lens, and consequently wreak havoc on the amplified pulse [4].

This thesis focuses on identifying, measuring, and understanding this thermal lensing phenomenon. Starting with simplified models, experiments will be conducted to try to find ways to identify and measure the effects of thermal lensing in various media and compare the results to simple models.

2 Background

2.1 What is Light?

Since this thesis focuses mainly on thermal lensing, which is observed in laser amplifiers, we should first understand how lasers (and light, for that matter) work. Light can be interpreted in two ways, generally referred to as the wave nature of light and the particle nature of light. To look at the wave nature of light, we go back to Maxwell's equations from electrodynamics. In a vacuum, Maxwell's equations read:

$$\nabla \cdot \mathbf{E} = 0 \quad (2-1)$$

$$\nabla \times \mathbf{E} = -\frac{\partial \mathbf{B}}{\partial t} \quad (2-2)$$

$$\nabla \cdot \mathbf{B} = 0 \quad (2-3)$$

$$\nabla \times \mathbf{B} = \mu_0 \epsilon_0 \frac{\partial \mathbf{E}}{\partial t} \quad (2-4)$$

This set of equations, which is a coupled partial differential equation, may be decoupled by taking the curl of (2-2) and (2-4). For the electric field, we get

$$\nabla \times (\nabla \times \mathbf{E}) = \nabla(\nabla \cdot \mathbf{E}) - \nabla^2 \mathbf{E} = -\mu_0 \epsilon_0 \frac{\partial^2 \mathbf{E}}{\partial t^2}, \quad (2-5)$$

and substituting (2-1) gives

$$\nabla^2 \mathbf{E} = \mu_0 \epsilon_0 \frac{\partial^2 \mathbf{E}}{\partial t^2}. \quad (2-6)$$

Likewise, for the magnetic field,

$$\nabla \times (\nabla \times \mathbf{B}) = \nabla(\nabla \cdot \mathbf{B}) - \nabla^2 \mathbf{B} = -\mu_0 \epsilon_0 \frac{\partial^2 \mathbf{B}}{\partial t^2}, \quad (2-7)$$

and substituting (2-3) gives

$$\nabla^2 \mathbf{B} = \mu_0 \epsilon_0 \frac{\partial^2 \mathbf{B}}{\partial t^2}. \quad (2-8)$$

Both of these equations fulfill the wave equation, $\nabla^2 \mathbf{A} = \frac{1}{\nu^2} \frac{\partial^2 \mathbf{A}}{\partial t^2}$. This means that electromagnetic radiation, which includes light, travel as a wave with amplitudes orthogonal to the direction of travel. This wave nature of light is how we interpret such phenomenon as polarization, interference, and refraction [1].

The derivation of particle nature of light was inspired by blackbody radiation and the photoelectric effect. In the case of blackbody radiation, classical physics could not describe the energy density of blackbody radiation at high frequencies. Max Planck solved the problem by treating the electromagnetic radiation as discrete bundles called *quanta*. These *quanta*, or *photons*, have a given energy, which is dependent on frequency, ν , and Planck's constant, h :

$$E = h \nu. \quad (2-9)$$

The observed photoelectric effect led to a similar problem. When bombarding certain metals with light, electrons would be emitted with a maximum energy that was measured as a voltage. This maximum kinetic energy was not dependent on the intensity of the incident light as classical models would have predicted, but was dependent on the frequency of the incident light. Again, the theory of discrete energy bundles explained the observations. The energy of a photon was needed to overcome the *work function* of the metal. If the frequency, and hence energy, was too low, an electron would not be liberated. If the frequency was high enough an electron would be liberated and any additional energy would be added to the electron's kinetic energy, increasing the voltage.

The quantum interpretation proves very useful. It is instrumental in the explanation of atomic transitions which make lasers possible. Using the Bohr model of hydrogen, which quantized angular momentum much like the quantization of the energy of light, we can start to explain atomic transitions. This can be shown by setting the Coulomb force equal to the centrifugal force of an electron around the nucleus:

$$\frac{Ze^2}{r^2} = \frac{mv^2}{r}. \quad (2-10)$$

Here, Z is the number of protons in the nucleus, r is the distance between the nucleus and the electron, m is the mass of an electron, v is velocity, and e is the elementary charge.

Bohr postulated that angular momentum, L , was quantized, and given by

$$L = mvr = \frac{nh}{2\pi}, \quad (2-11)$$

where n is an orbital level, and h is planck's constant. Solving (2-11) for m and plugging into (2-10) and then solving for v yields

$$v = \frac{2e^2 Z \pi}{hn}. \quad (2-12)$$

Now, plugging (2-12) into (2-10) and solving for r leads to

$$r = \frac{n^2 h^2}{4me^2 Z \pi^2}. \quad (2-13)$$

Knowing that total energy is the sum of kinetic energy and potential energy,

$$E = T + U = \frac{mv^2}{2} - \frac{Ze^2}{r}, \quad (2-14)$$

we can plug (2-12) and (2-13) into (2-14) and get

$$E_n = -\frac{2\pi^2 e^4 Z^2 m}{h^2 n^2}. \quad (2-15)$$

This formula shows that the energy is quantized by an integer n , which corresponds to the orbital level. A transition from a higher level to a lower level will lead to an energy difference given by

$$\Delta E = E_i - E_f = -\frac{2\pi^2 e^4 Z^2 m}{h^2 n_i^2} - \left(-\frac{2\pi^2 e^4 Z^2 m}{h^2 n_f^2}\right) = -\frac{2\pi^2 e^4 Z^2 m}{h^2} \left(\frac{1}{n_i^2} - \frac{1}{n_f^2}\right). \quad (2-16)$$

This energy difference manifests itself as an emitted photon. Plugging (2-9) in for ΔE leads gives us an expression for the frequency of the photon emitted for a specific atomic transition:

$$h\nu = E_i - E_f = -\frac{2\pi^2 e^4 Z^2 m}{h^2} \left(\frac{1}{n_i^2} - \frac{1}{n_f^2}\right). \quad (2-17)$$

This formula works for hydrogen, but must be modified for other elements due to additional forces, resulting in more energy terms. To correct this, the $-\frac{2\pi^2 e^4 Z^2 m}{h^2}$ term varies for each element, making (2-17)

$$h\nu = E_i - E_f = -R \left(\frac{1}{n_i^2} - \frac{1}{n_f^2}\right), \quad (2-18)$$

where $-R$ is the Rydberg constant which varies for different elements [2].

2.2 The Laser

The laser, which is an acronym for light amplification by stimulated emission of radiations, is the result of atomic transitions and a quantum mechanical idea called *stimulated emission*. Stimulated emission means that if an electron is in an excited level

and a photon of energy equal to the energy difference between the excited and the lower state hits the atom, then there is a probability that it will stimulate the emission of a photon of equal frequency, phase, and direction. There are two other process which we must look at. The first is *spontaneous emission*, which means there is a probability that an electron in an excited state will randomly decay to the lower state, emitting a photon in any direction. The second is *stimulated absorption*. This means that an electron in the lower state has a probability of being excited up to a higher state if hit with a photon of sufficient energy. We can look at this in a simplified way to see what is necessary to get amplification by stimulated emission. If we say that the stimulated emission from the upper level to the lower level is equivalent to the stimulated absorption from the lower level to the upper level, then the system would be in equilibrium, i.e. there is no amplification:

$$N_u p_{ul} = N_l p_{lu}. \quad (2-19)$$

Here, N_u and N_l are the upper and lower populations respectively and p_{ul} and p_{lu} the probabilities of stimulated emission and stimulated absorption respectively. In order to amplify the light, we must have more stimulated emissions than stimulated absorption,

$$N_u p_{ul} > N_l p_{lu}. \quad (2-20)$$

This can be rewritten as,

$$N_u > \frac{p_{lu}}{p_{ul}} N_l. \quad (2-21)$$

From this expression, we can conclude that in order to get light amplification from stimulated emissions, we must have a higher upper level population than lower level

population by some factor dependent on the absorption and emission probabilities. This is generally referred to as *population inversion*.

In order to achieve population inversion, we must pump the electrons to the upper level. The most common way is to optically pump the electrons to the upper level by stimulated absorption of photons. The traditional three-level system diagram is shown below.

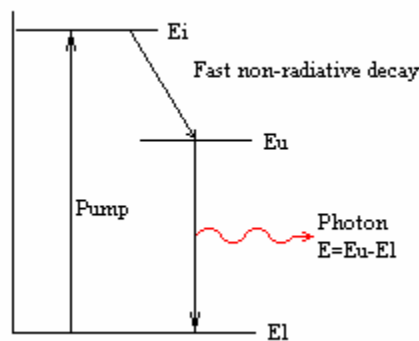


Figure 1: This diagram shows the traditional three-level system. There are three distinct energy levels defined by E_l , E_u , and E_i . The electron is pumped to the unstable E_i state where it undergoes a fast non-radiative decay. The E_u to E_l transition emits a photon by stimulated emission with energy $E = E_u - E_l$.

The electrons start in the lower state, E_l , which is on the bottom of the diagram. The electrons are then pumped up to a short lifetime level, E_i , where they quickly decay via a non-radiative decay to the upper level E_u which is said to be *metastable*. This *metastable* state has a long lifetime, leaving time for stimulated emission to occur. From this level, the electron will decay to the lower level, either by stimulated or spontaneous emission, emitting a photon.

Another thing needed to achieve light amplification is a proper cavity. By placing mirrors on either side of the *lasing medium*, the light will reflect back and forth, further producing stimulated emission. The *lasing medium* is the material that contains the

atoms which will be excited and undergo stimulated emission. Consequently, the only photons which will be able to exist in this cavity are those which form a standing wave. This is because electromagnetic theory says that in order for electromagnetic waves to be supported or enhanced, the wave must be zero at the boundaries of the cavity. The following equation tells us which wavelengths will exist as a function of cavity length

$$\lambda_n = \frac{2l}{n} \quad (2-22)$$

where l is the cavity length and n an integer referring to the mode of the wave. By only partially silvering one of the cavity mirrors, coherent light is allowed to escape, creating a laser beam.

2.3 The Laser Oscillator

The laser we just looked at is what we would generally call a *Continuous Wave laser*. This means that the laser is a continuous, typically monochromatic wave, i.e. only one wavelength. There is another type of laser which can run as a CW laser and can emit multiple wavelengths in pulses. This type of laser is known as a *laser oscillator*. In this case, the lasing medium will amplify a spectrum of wavelengths, so long as they satisfy equation (2-22) to exist in the cavity. As a result, a stream of pulses can be emitted if these modes can be put in phase. We can observe how this occurs by looking at a few modes which can exist in the cavity with different phase.

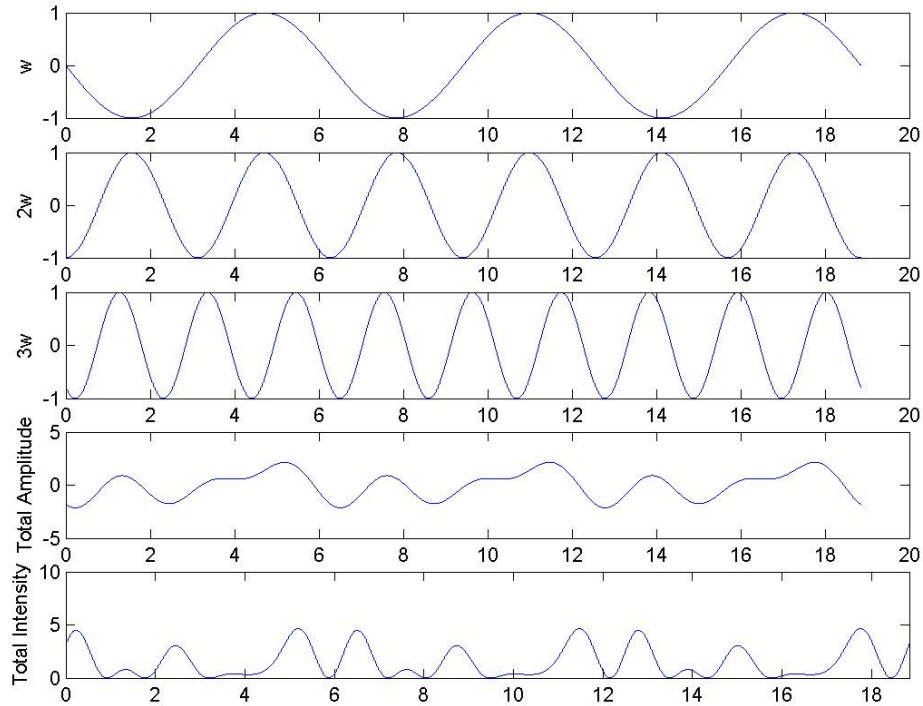


Figure 2: This figure shows three different waves which are out of phase. The superposition of their amplitudes gives the total amplitude. The square of this amplitude gives us the intensity of the combined wave.

By combining the amplitudes of the different modes, we can see what the total electric field would look like and by squaring the sum of combined amplitude we see the intensity of the electric field.

Now let us look at the same thing, but with the modes in phase.

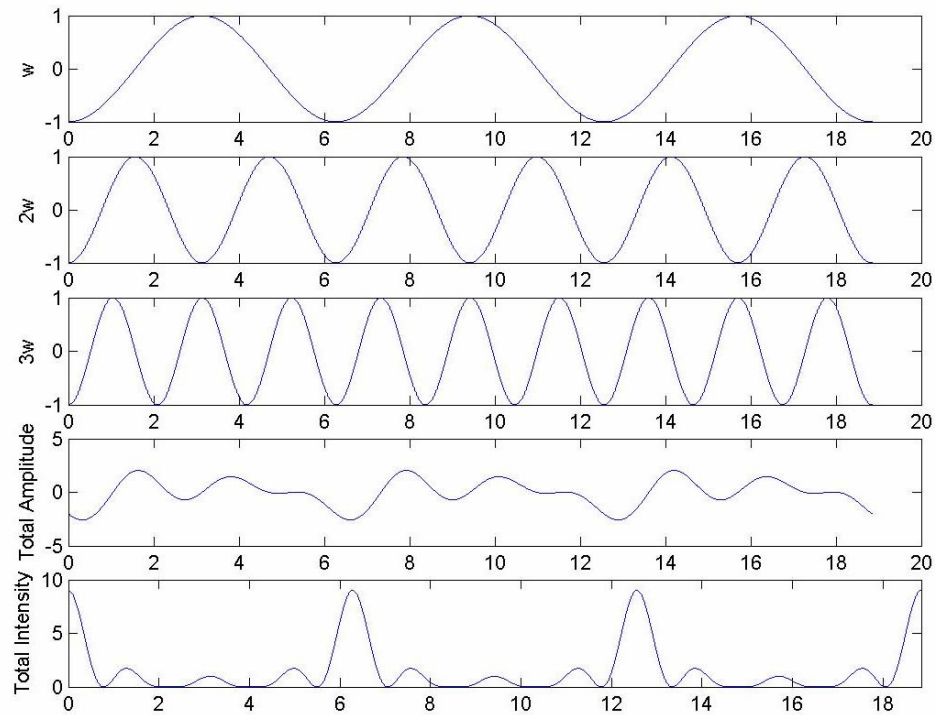


Figure 3: This figure shows three different waves which are in phase. The superposition of their amplitudes gives the total amplitude. The square of this amplitude gives us the intensity of the combined wave. When the waves are in phase they construct much higher peak intensities.

Note in figure 3 how the intensity is much larger when the waves are in phase. By adding these distinct frequencies in phase we are *mode-locking* the laser. The more frequencies we are able to produce, the shorter the output pulses. Many times, these pulses are on the order of femtoseconds (10^{-15} s). The pulses produced in our lab run at roughly 10 fs, which corresponds to a spatial length along the propagation direction of $3\mu\text{m}$ per pulse.

The method which the oscillator in our lab uses for mode locking is called *Kerr lensing*. Kerr lensing is a phenomenon which causes an instantaneous change in index of refraction due to the intensity of light traveling through the medium. By focusing the pump beam on the lasing medium, titanium sapphire crystal (Ti:sapph) in our case,

preferential treatment will be given to the pulsed mode. This is because the pulsed mode has a higher intensity, which will be focused more due to Kerr lensing. Being focused will cause more of the pulsed beam to travel through the pumped lasing medium than the normal CW-mode. This will make the pulsed mode stronger than the CW-mode and will in turn further reduce the CW-mode until the pulsed mode dominates. The picture below helps show how the narrow pump beam gives preference to the pulsed mode due to its higher intensity [3].

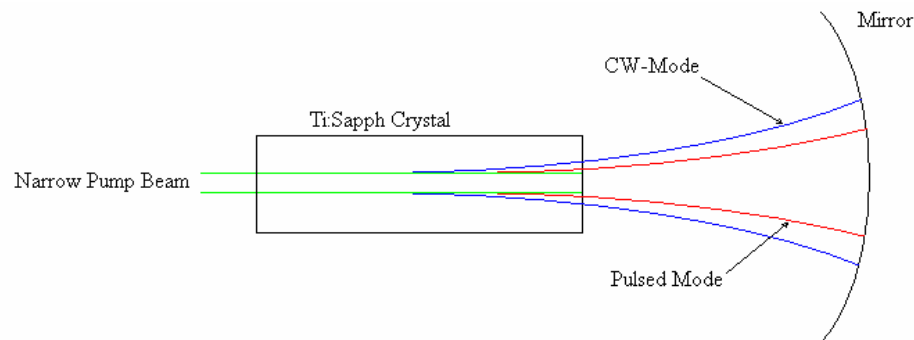


Figure 4: This figure shows how Kerr lensing causes mode-locking. When a pulsed mode, which can be created by changing the cavity length, enters the crystal, its higher intensity causes the Kerr lensing effect. The less intense CW mode doesn't induce this Kerr lensing so is left to diverge more. Since the pulsed mode is focused it will pass through more of the narrow pumped crystal than the CW mode, causing the pulsed mode to be amplified more and eventually driving the CW mode to zero.

2.4 Chirped Pulse Amplification

In order to make the ultra-short pulses from the laser oscillator usable for physics experiments, they must be further amplified. The method used is known as chirped pulse amplification. First, a pulse from the oscillator is picked out of the stream of pulses.

This pulse is then stretched out in time, making its duration much longer than the original 10 fs. It is required that the pulse be stretched out to lower the intensity going through the lasing medium at a given time.

The pulse is stretched either by diffraction gratings or prisms. Diffraction gratings, as seen in figure 5, allow all of the different frequencies of the pulse to be separated. Once separated, the different colors can be sent different distances in space, so that when they are recombined using a diffraction grating, the colors are offset in time.

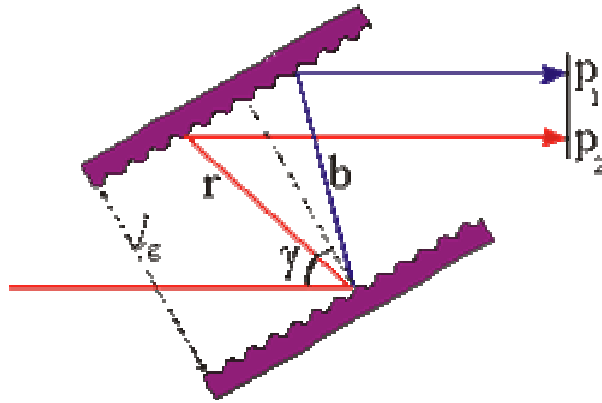


Figure 5: This figure shows a diffraction grating type pulse stretcher. When a pulse hits the first diffraction grating, the different frequencies are spread out at different angles. Upon hitting the next grating, the different colors are made parallel again. The colors are then retro-reflected back through the two gratings, recombining them with a temporal phase change. This phase change can be controlled by sending the different colors differing distance. (picture from <http://dutch.phys.strath.ac.uk/FRC/stuff/dictionary/dictionary.html>)

The same thing can be done with prism, figure 6, but now refraction is used to separate the colors. By changing the distances the different colors travel in air and in glass, the pulse can be stretched out in time.

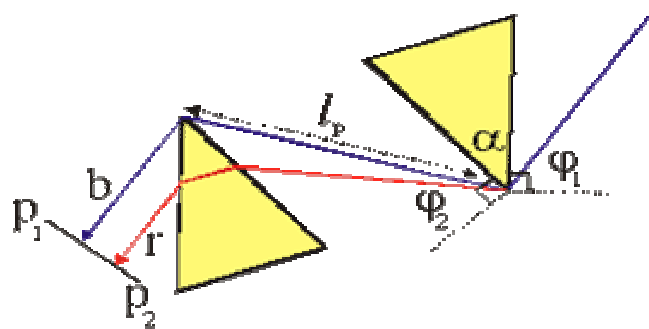


Figure 6: This figure shows a prism pair type pulse stretcher. When a beam hits the first prism, the different frequencies are refracted at different angles. The different frequencies then encounter another prism which refracts the respective colors parallel again. The colors are then

retro-reflected back along the same path, further spreading the pulse in time. The spreading may be controlled by varying the respective paths of the different colors in air and in glass, by moving a prism in or out of the beam path. (picture from <http://dutch.phys.strath.ac.uk/FRC/stuff/dictionary/dictionary.html>)

After the pulse has been stretched out, it is sent into an amplification scheme.

Two different schemes are generally used, the regenerative amplifier and the multi-pass amplifier. The regenerative amplifier uses a pair of concave mirrors which create a stable cavity for the beam to pass back and forth through the lasing medium. A difficulty with this design is getting the pulse into and out of the cavity. This is usually done using optical switches, called Pockel cells, and a polarizer. This method causes problems for ultra-fast pulses, because the repeated passes through the Pockel cells stretch out the pulse, making it harder to recompress.

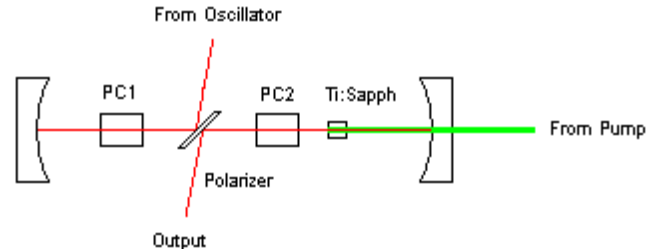


Figure 7: This figure shows a regenerative type amplifier. A pulse is input into the cavity and reflected off a polarizer. It then passes through a Pockel cell. This Pockel cell will rotate the polarization so that the pulse will remain in the cavity until the Pockel cell rotates the polarization back to a direction that the amplified pulse can be reflected out of the cavity.

The other method, the multi-pass amplifier, uses clever geometries to deliver multiple passes without the use of optical switches. This allows much easier, and more controlled, recompression.



Figure 8: This figure shows a simple multi-pass type amplifier. The pulse is repeatedly reflected through the lasing medium using clever geometries. This scheme eliminates the need for optical switches, making pulse recompression much easier.

A drawback to this design is choosing in the number of passes through the lasing medium. This can easily be controlled in the regenerative amplifier, by simply changing the timing of the Pockel cells. In the multi-pass amplifier, the entire scheme must be rebuilt in order to change the number of passes through the lasing medium [4].

3 Thermal Lensing

To pump the electrons in the laser crystal up to the upper level, a tremendous amount of optical energy must be used. The absorption of the optical energy from the pump causes heat to build up in the crystal. Heat in the crystal causes small changes in the optical properties as well as the shape of the crystal itself. These optical changes cause the crystal to form a tiny lens which will focus the light traveling through it. In an amplification scheme with many passes through the crystal, this tiny lens will cause the beam to diverge so that it can no longer be amplified.

Thermal lensing is the result of two material changes. The first is a temperature dependence on the index of refraction. The second is a temperature dependent curvature of the face of the material. Moreover, the index of refraction change due to temperature contains two components. One is a pure index change from the thermo-optic coefficient,

$\frac{dn}{dT}$, and the other a more complex stress-dependent variation which depends on

direction-dependent elasto-optical coefficients. When all the components are assembled, a focal length prediction can be made for cylindrical optical structures, such as a laser rod:

$$f = \frac{KA}{P_h} \left(\frac{1}{2} \frac{dn}{dT} + \alpha C_{r,\phi} n_0^3 + \frac{\alpha r_0 (n_0 - 1)}{l} \right)^{-1}. \quad (3-1)$$

Here, K is the thermal conductivity, A is the cross sectional area of the medium, P_h is the heat dissipated, $\frac{dn}{dT}$ is the thermo-optic coefficient, α is the coefficient of thermal expansion, $C_{r,\phi}$ are functions of the elasto-optical coefficients for the material, n_0 is the index of refraction at the center of the rod, r_0 is the radius of the rod, and l the length of the rod. The complete derivation of this formula may be found in *Solid-State Lasers* by Koechner and Bass[5]. The dominant term in this expression is that of the temperature dependent index of refraction. So, we will simplify (3-1) to

$$f = \frac{KA}{P_h} \left(\frac{1}{2} \frac{dn}{dT} \right)^{-1}. \quad (3-2)$$

This equation allows us to predict the focal length of a thermal lens in a cylinder as a function of absorbed pump power. If we plug in the constants for a 0.25” diameter sapphire, with $K = 36 \frac{W}{m^\circ K}$, $A = 0.00003167m^2$, and $\frac{dn}{dT} = 1.4 \times 10^{-5} \frac{1}{^\circ K}$, we find that

$$f = \frac{162.87}{P_h}. \quad (3-3)$$

Generalized, this means that we should see that the focal length of a thermal lens is inversely proportional to the absorbed pump power.

4 Experiments and Results

4.1 Interferometric Imaging of Thermal Lens in Glass

The first experiment to be conducted was to view the thermal lens using an interferometric technique. When a microscope slide is illuminated at an angle with a Helium Neon laser, an interference pattern can be observed. This interference pattern is due to the wave-like nature of light. When two waves of differing phase coincide, they produce constructive or destructive interference. In this case the light reflecting off the front of the microscope slide is interfering with the light reflecting from the back of the microscope slide.

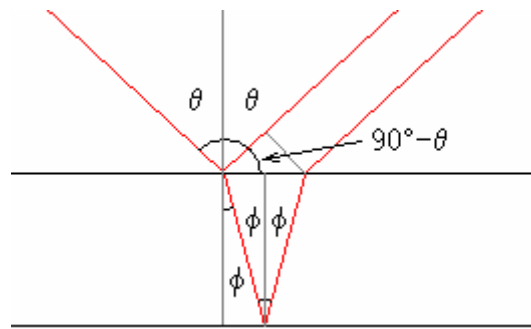


Figure 9: This figure shows how the interference pattern is created. The first beam is reflected off the surface while another portion of the beam travels into the medium, is reflected off the back surface, and then comes back out.

If the slightest change in the glass occurs, be it thermal expansion, change in index of refraction, or a combination of both, the path length for the light reflected off the back of the microscope slide will change, causing a shift in the interference pattern.

To perform this experiment, a few devices had to be constructed. First, a device had to be constructed to hold the microscope slide which would interface with our existing optics posts. This custom microscope holder was made of aluminium in the student machine shop.



Figure 10: This figure shows the custom-made microscope slide holder constructed to mount on our existing optics posts.

Another device had to be constructed to help align the two laser beams that would eventually be used in all experiments. This was simply a microscope slide sized piece of aluminium with a tiny hole drilled and countersunk in the center.

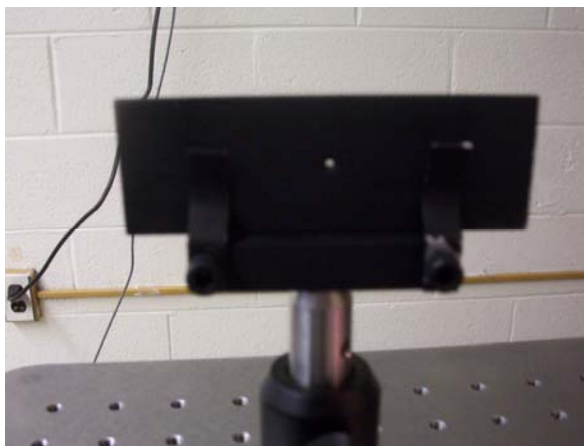


Figure 11: This figure shows the custom made alignment tool in the holder.

The setup for the experiment consisted of two lasers. The first was the pump laser which would actually be used to form the thermal lens. It was a Positive Light Evolution

30, Q-switched, diode pumped, frequency doubled Nd:YAG laser, with output of 532nm, which is in the green. Q-switching uses optical switches to turn the lasing cavity on and off at around 1 kHz. By doing this, pulses are emitted at 1 kHz, with much higher intensities than when the laser is not Q-switched. The second laser was a simple Metrologic Helium Neon laser (HeNe) which was used as a coherent source to probe for the thermal lens.

The Nd:YAG pump laser was focused down using a 100mm focal length lens and terminated in a Moletron PM150-50 laser power meter. The alignment tool was placed in the microscope slide holder and placed at the focus of the laser so that the focus coincided with the hole in the center of the alignment tool. The HeNe was then set up using a mirror to reflect the beam through the same hole in the alignment tool, though the beam was too large to fully pass through.

Once both lasers were aligned, the alignment tool was removed from the microscope slide holder and replaced with a glass microscope slide. The interference pattern could be found in the reflection of the HeNe laser off the microscope slide. A Sony Super HAD CCD SSC-M183 camera was then placed in the path of the interference pattern so that the pattern could be imaged. A green blocking filter was placed in front of the camera to block the scattered green light from the pump laser.

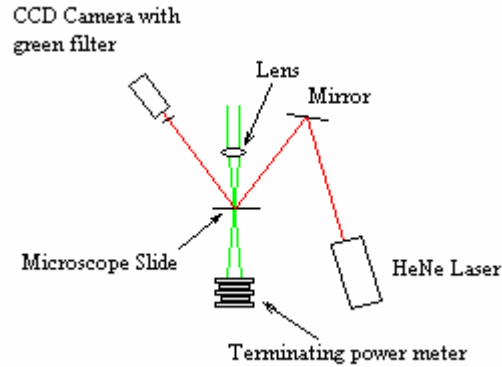


Figure 12: This figure shows the layout the interferometric imaging setup.

The camera was then connected to a computer using an Osprey video capture card running Labview 7 software so that the images could be saved.

An initial image was taken of the interference pattern with the Nd:YAG pump laser off. This image gives us a baseline to detect any shift in the interference pattern. A series of images were taken of the interference pattern at varying laser intensities, starting with the minimum energy of 10 amps of diode current, which pump the green laser. At each level of diode current, an image was taken, transmitted power recorded via the terminating power meter, and the diode current recorded. This was repeated at intervals from 10 to 20 A of diode pump power.

The image file recorded from the CCD camera is a matrix of numbers referring to the intensity recorded from each CCD sensor on the camera's chip. Our camera contains an array of 510 X 492 individual CCD pixels on a 4.8 mm by 3.6 mm chip, though the image is converted to either a 640 X 480 or a 320 X 240 matrix when saved to the computer. Since the resulting image is simply a matrix of numbers, comparisons between images is very easy. To look for a shift in the interference pattern, the baseline image could be subtracted from the image to be analyzed. The matrices for the respective

images were loaded into Matlab. Using this program, the matrices could easily be subtracted and then the composite image plotted.

4.1.1 Interferometric Imaging of Thermal Lens in Glass Results

The raw images at high pump powers show obvious shifts, indicating some optical change attributed to thermal lensing. At these high power levels we can see warping in the fringe lines, but it is difficult to interpret. Once we look at the composite images by combining an image with the initial image, the changes become more apparent. At very low powers there is not much change at all. In fact, at 10 amps there is almost no change in the glass because the two images nearly cancel out perfectly. At around 11 amps, we can see that there is a localized fringe shifted near the center of the image. By 12 amps, we can see that nearly the entire fringe pattern has shifted. At 13 amps we can see there is a circular fringe pattern emerging, which is indicative of lenses. From 13-20 amps, we continually see added fringes, meaning that there is an ever increasing optical change occurring in the glass.

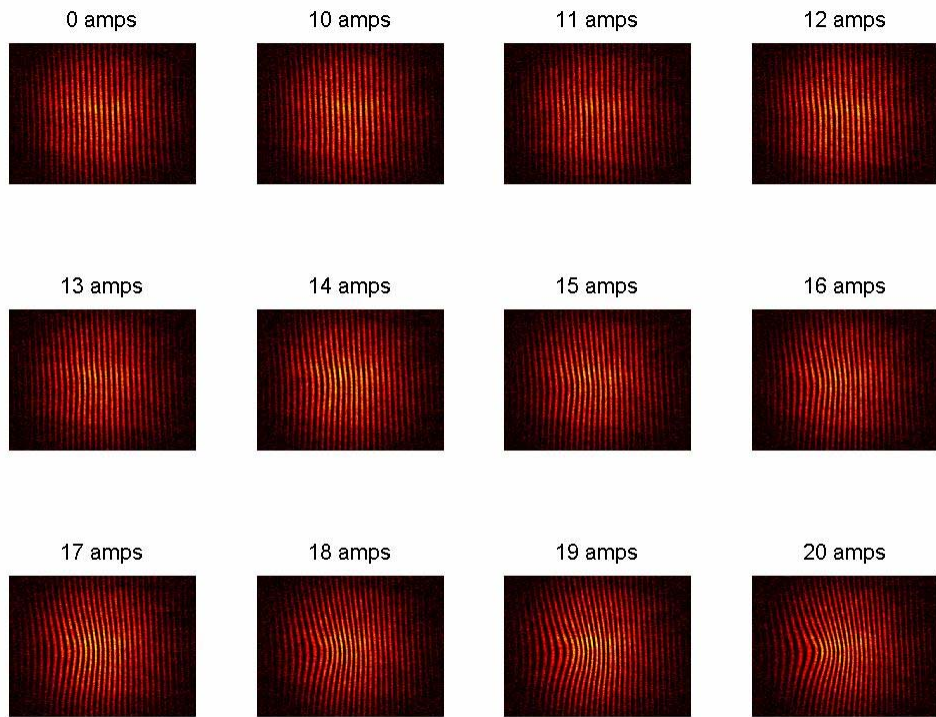


Figure 13: This figure shows the raw data from the CCD camera. We can see the evolution of the fringe shifts as diode pump current is increased. Low powers only show a slight shift if any at all, but at high powers we see warping of the fringe lines.

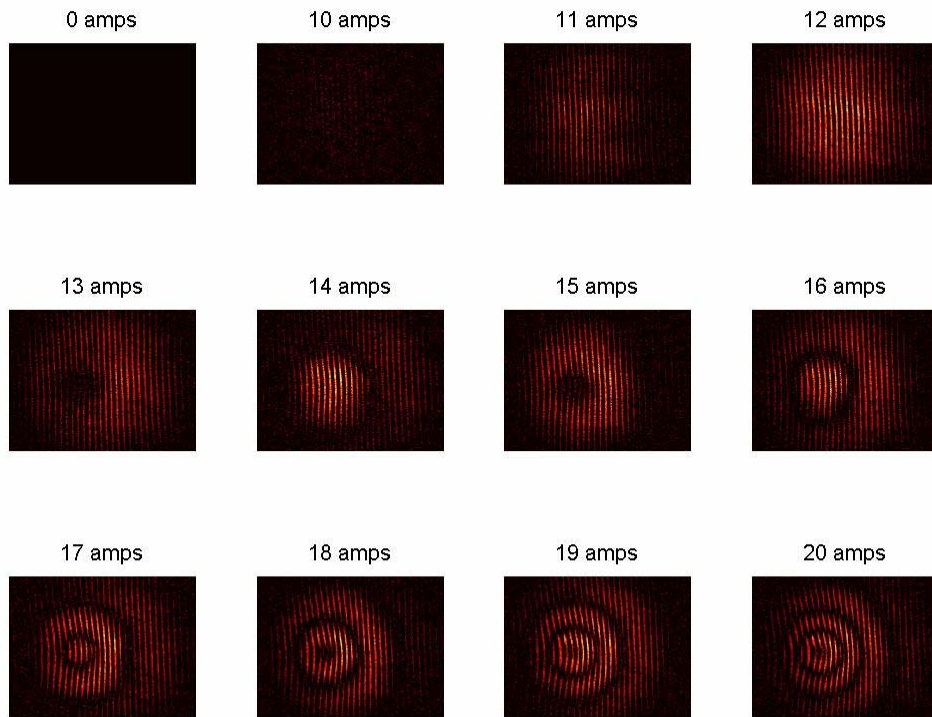


Figure 14: Once we combine the images with the initial image, we can see the slightest change in the interference pattern. At low powers we see a shift in the fringe pattern. At higher powers we see the circular fringes which are indicative of lenses.

4.2 Focusing due to Thermal Lens in Glass

For this experiment, we used nearly the same setup as the interferometric imaging experiment. Trying to image the focus meant that the CCD camera had to be moved to look at the transmitted portion of the HeNe laser beam as opposed to the reflection. The green filter in front of the camera was also replaced with a medium and a low density filter in series. The distance from the microscope slide to the camera was carefully measured and recorded to make it possible to extrapolate the focal length of the thermal

lens. A spectral-physics 407ATC power meter was also set up to record the reflected pump intensity.

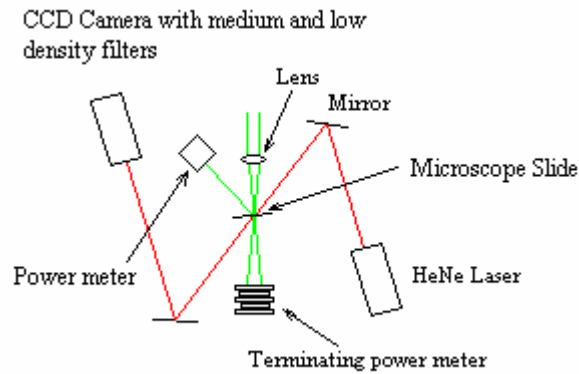


Figure 15: This figure shows the layout of the focus measuring setup.

A procedure similar to interferometric imaging was used for recording data. With the laser off and at each pump diode current from 10-20 amps, an image was saved, terminating laser power recorded, and also reflected pump power recorded. Recording both the reflected and transmitted pump power made it possible for us to find the total energy absorbed in the microscope slide.

Once all of the data was taken, a row in the center of the image was chosen, corresponding to a cross-section in the middle of the beam. This data was then plotted and a fit with a gaussian. A width parameter was taken from the gaussian fit. This parameter corresponded to the half width at $\frac{1}{e^2}$, e being the exponential. This width would correspond to the width in terms of pixels, or cells of the image matrix. In this case, the image matrix was 320 X 240. Since we know that the chip of the Sony CCD camera is 4.8mm X 3.6mm we can find the actual width of the beam which was on the

camera. From this actual width and measured length to the thermal lens, we can estimate the focal length of the thermal lens by using similar triangles.

4.2.1 Focusing due to Thermal Lens in Glass Results

The images of the thermal lensing were very dramatic. At 11 amps of diode pump current focusing could already be seen. As the current continued to be raised the spot simply got smaller and smaller with greater intensity.

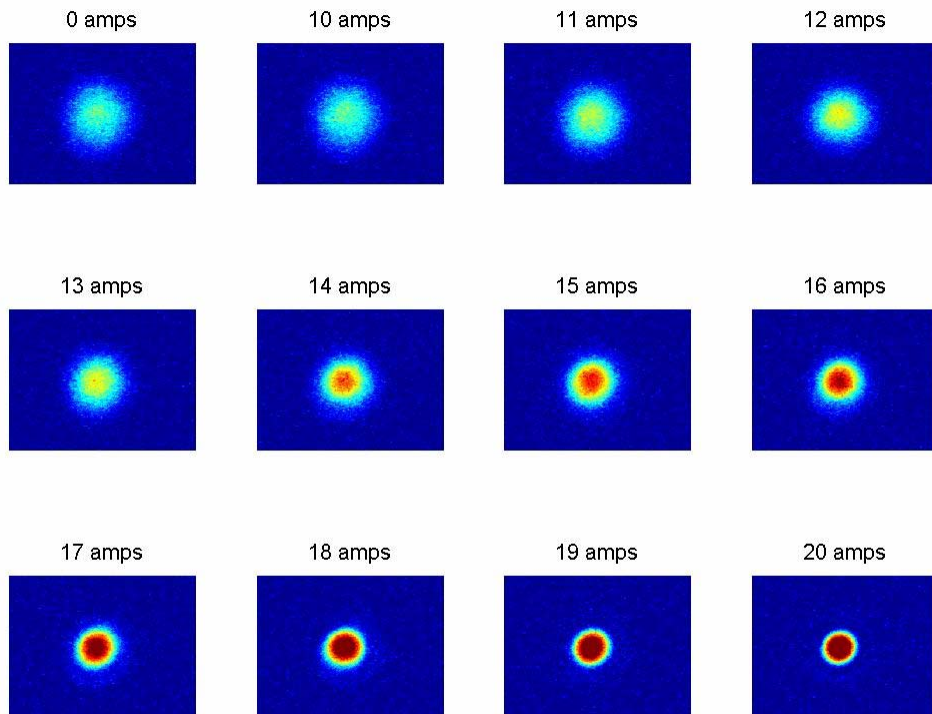


Figure 16: This figure shows the evolution of the beam through a thermal lens with varying pump intensity.

Using similar triangles, we were able to estimate the focal length of the thermal lens.

| Pump Diode Current | 1/e ² width (pixels) | waist (m) | Total Power (W) | Terminating Power (W) | Reflection (W) | Absorption (W) | focal length (m) |
|--------------------|---------------------------------|------------|-----------------|-----------------------|----------------|----------------|------------------|
| 0 | 74.34 | 0.00055755 | 0 | 0 | 0 | 0 | infinity |
| 10 | 76.012 | 0.00057009 | 0.0593 | 0.0567 | 0.006 | -0.0034 | error |
| 11 | 72.472 | 0.00054354 | 1.01 | 0.92 | 0.072 | 0.018 | 26.6637045 |
| 12 | 66.834 | 0.00050126 | 2.29 | 2.09 | 0.18 | 0.02 | 6.63573141 |
| 13 | 62.139 | 0.00046604 | 3.86 | 3.53 | 0.3 | 0.03 | 4.08227194 |
| 14 | 56.071 | 0.00042053 | 5.68 | 5.16 | 0.42 | 0.1 | 2.72635612 |
| 15 | 55.932 | 0.00041949 | 7.61 | 6.89 | 0.55 | 0.17 | 2.70576923 |
| 16 | 48.861 | 0.00036646 | 9.5 | 8.64 | 0.69 | 0.17 | 1.95485694 |
| 17 | 45.383 | 0.00034037 | 11.6 | 10.4 | 0.84 | 0.36 | 1.72006078 |
| 18 | 42.294 | 0.00031721 | 13.7 | 12.4 | 1.1 | 0.2 | 1.5542595 |
| 19 | 37.613 | 0.0002821 | 15.9 | 14.3 | 1.3 | 0.3 | 1.35616304 |
| 20 | 34.24 | 0.0002568 | 18.2 | 16.4 | 1.4 | 0.4 | 1.24208978 |

Figure 17: This figure shows the data taken and the extrapolated focal lengths.

The measured values were plotted versus the absorbed pump power. We can see in the

graph below that when the data is compared to the function $f(x) = \frac{0.2}{x}$ we get a very

close match. This matches the expected inverse proportionality of focal length and

absorbed pump power from a cylindrical optic element (see eq. 3-3).

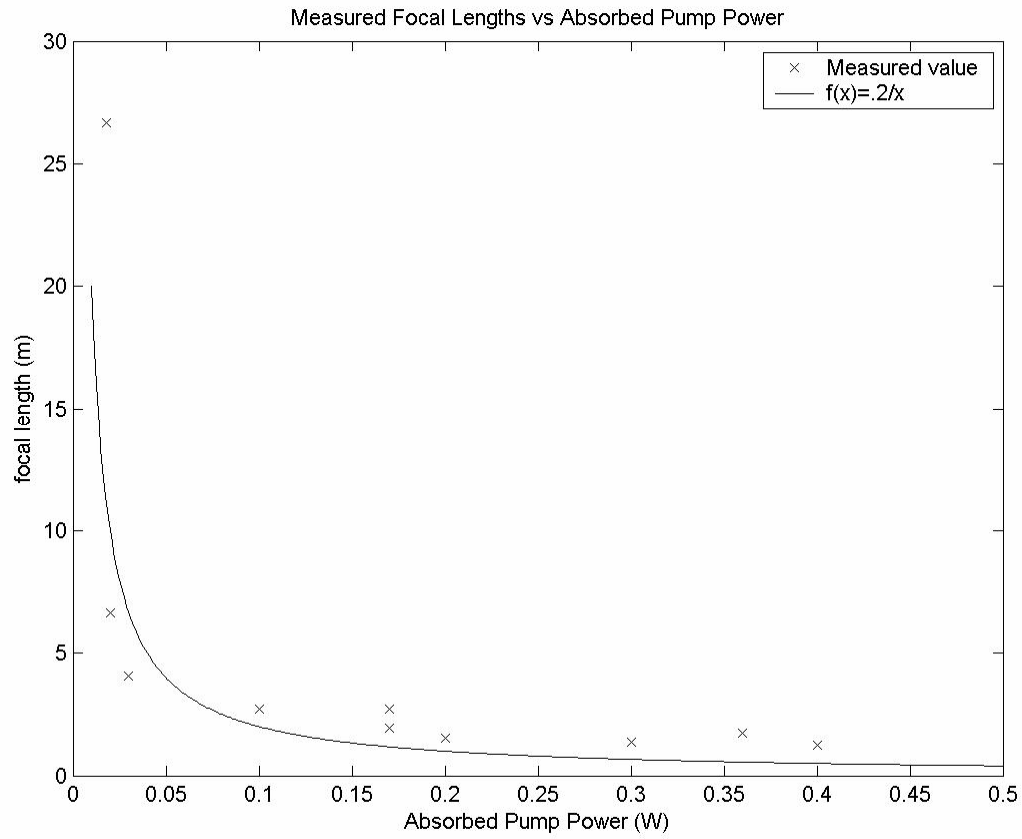


Figure 18: This figure shows the focal lengths plotted versus absorbed pump power. In this plot a $\frac{0.2}{x}$ curve was plotted to show the inverse proportionality of focal length and absorbed pump power.

4.3 Focusing due to Thermal Lens in Sapphire

In order to better simulate thermal lensing in Ti:sapph, we decided to look at normal sapphire crystal. This was a much cheaper alternative to the actual material, as Ti:sapph is very expensive. An adequate source of sapphire was found in small .25” diameter by .125” thick vacuum chamber windows.

Like the microscope slide, a way had to be devised to hold the sapphire crystal. Again a precision custom mount was fabricated. This mount was made of copper for its

favorable thermal properties since it was also designed to be chilled via a liquid flowing through the base if ones so chose. To further increase the thermal contact, CPU thermal paste was used to bond the crystal to the mount as well as the two halves of the mount together. The idea behind this design was to try to cool the crystal to reduce the thermal lensing observed.

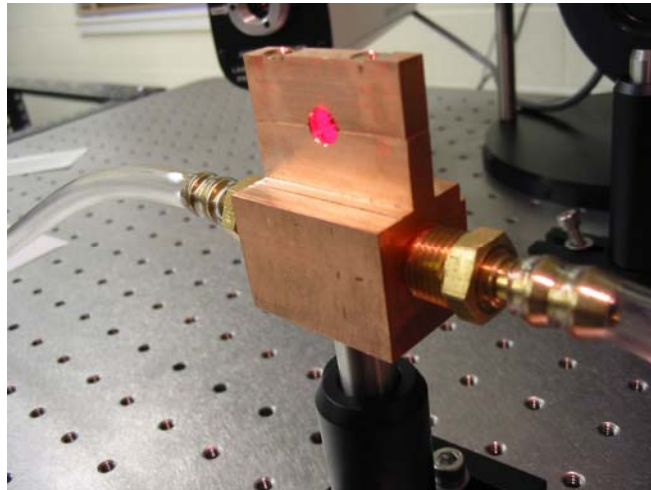


Figure 19: This figure shows the custom, copper crystal mount made to mount on our existing optics posts. The mount was also designed to have liquid cooling capabilities.

The setup for this experiment was the exact same as the focusing experiment in the microscope slide except the microscope slide and holder was replaced with the crystal mount and sapphire crystal.

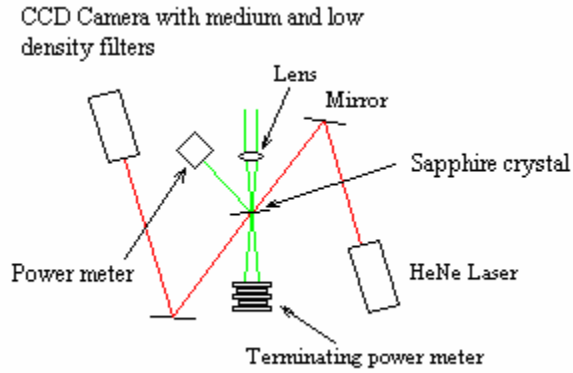


Figure 20: This figure shows the layout of the focus measuring setup.

4.3.1 Focusing due to Thermal Lens in Sapphire Results

Once the pump laser was turned on, there was a surprising effect observed in the sapphire. While wearing goggles that blocked the green light of the pump laser, we observed a red fluorescence in the sapphire. This fluorescence is due to an atomic transition in the sapphire caused by excitation from the pump laser. It is not known which atoms fluoresced, and it is not in the scope of this experiment, but it was an interesting observation nonetheless.

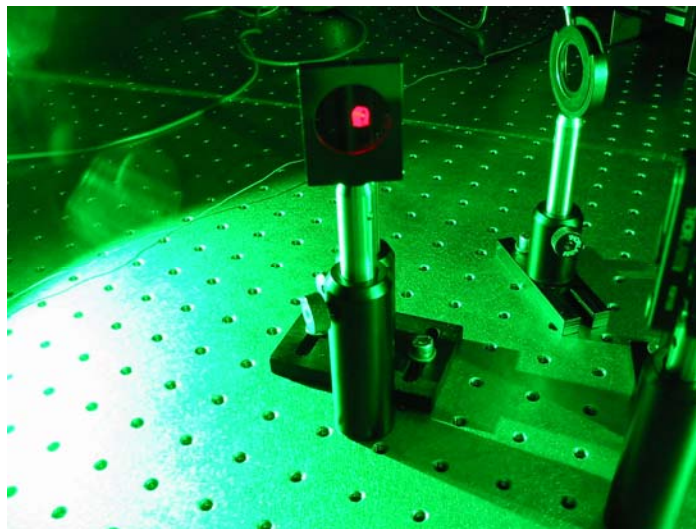


Figure 21: This figure shows the un-mounted sapphire crystal fluorescing from optical pumping by the Nd:YAG laser. A green blocking filter is mounted in the foreground.

Unexpectedly, no focusing from thermal lensing was detected in the sapphire. This was surprising, even at 20 amps pump diode current, there was not the slightest bit of change in the image. It was thought that perhaps the laser beams were not aligned properly, so this was checked. Upon closer inspection, it was very easy to see that they were crossing because the path of the green beam was clearly visible due to fluorescence and the HeNe beam could easily be seen on either surface of the sapphire. It was thought that perhaps the thermal lensing was much weaker in the sapphire causing a much longer focal length lens. So, the CCD camera was placed a greater distance from the sapphire. This too detected no change in the optical characteristics of the sapphire. At this point it was concluded that a new method would have to be used to try to detect an optical change in sapphire.

4.4 Mach-Zehnder Interferometric Imagery

In order to try to detect a small optical change, a Mach-Zehnder interferometer was built. This type of interferometer uses two beam splitters. The first beam splitter splits the beam creating two distinct arms. Each beam is then reflected by a mirror to the second beam splitter, where they are recombined. This type of interferometer allowed us to probe a material in one arm and detect a change in the interference pattern when recombined with the unaltered arm. This method is very similar to the first technique used to image the microscope slide, but allows us to look at the sapphire also without the need of a reflection from the rear surface.

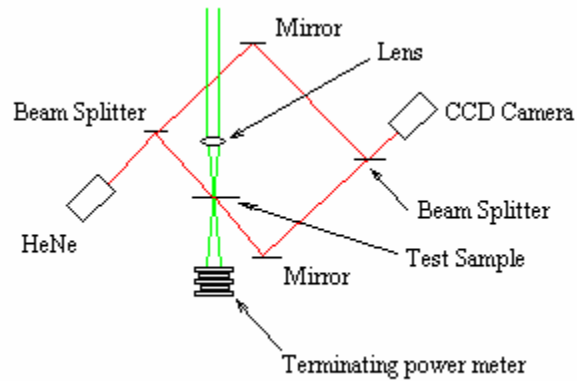


Figure 22: This figure shows the layout of the Mach-Zehnder Interferometer.

In order to test the setup, glass was placed in one arm of the interferometer. The diode pump power was turned all the way up to 20 amps so we could see how sensitive the interferometer was. There was surprisingly very little change in the image as pump power increased. To further look at the sensitivity of the interferometer, the microscope slide was replaced with a 100 mm focal length lens. The corresponding image only had a few circular fringes. Since the 100 mm focal length lens was much stronger than the thermal lensing we expected from either glass or sapphire, it was concluded that this interferometer was not sensitive enough to yield any useful information, but proved to be a good exercise in optical alignment.

4.5 Combination Interferometric Imagery

Knowing that both materials had very flat surfaces with some reflectance, a combination interferometric imagery technique was tried. This method used the Mach-Zehnder interferometer, but replaced one of the mirrors with the material to be probed.

An interference pattern of three separate beams would be observed. Two beams came from the reflection from the front and back of the microscope slide as in the first interferometric image experiment, while the third was the unaltered arm of the Mach-Zehnder interferometer. The CCD camera was placed in the path of the three coinciding beams with the medium density filter.

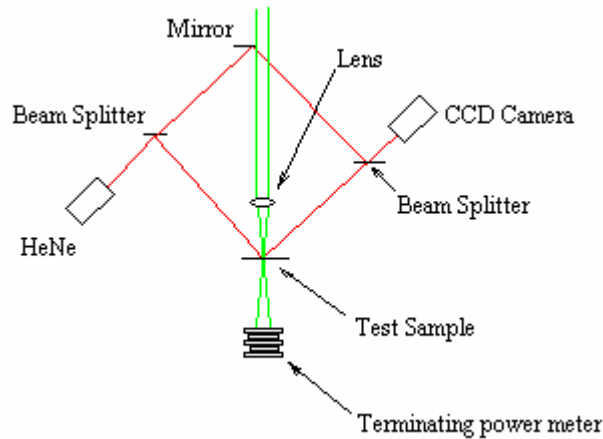


Figure 23: This figure shows the layout of the Combination Interferometer.

The standard procedure was followed of recording an image and terminating power for the pump diode currents from 10-20 amps. After looking at the microscope slide, the sapphire was then put into the interferometer and the system realigned and tested.

4.5.1 Combination Interferometric Imagery Results

The combination technique showed very interesting images. There was a pseudo linear interference pattern, which was due to a tilt in the microscope slide, visible in the initial image. When the pump laser was turned on, results were immediately apparent. The first few diode current settings, 10-14 amps, showed a shift of the linear interference pattern. Once diode current reached 15 amps, a circular pattern started to emerge and

began to dominate. This pattern evolved and eventually came to resemble a spiral galaxy. The cause for this pattern evolution isn't quite understood, as it is a complex interference of three separate beams. The linear pattern is most likely due to a slight tilt in the microscope slide, while the circular pattern is most likely a change in the index of refraction or distortion in the shape, both of which would give a circular shape.

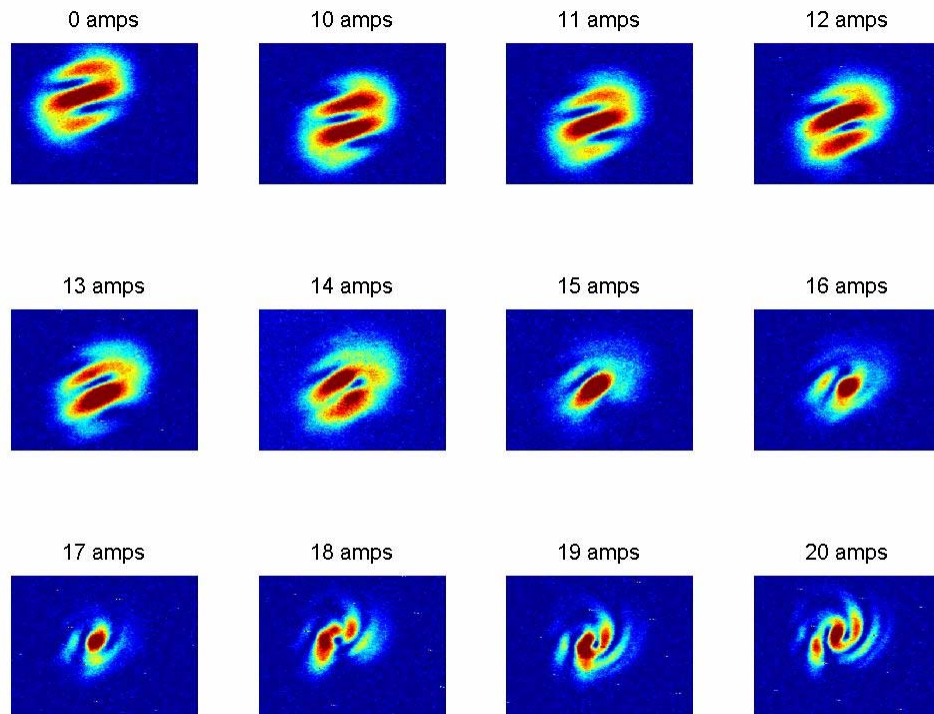


Figure 24: This figure shows the evolution of the combination interferometer interference patterns. Results are immediately apparent in the shift of the linear fringes. At higher pump powers, a circular pattern emerges creating a spiral interference pattern.

We then looked at the sapphire in this interferometer setup, hoping that it would be sensitive enough to detect an optical change in the sapphire. Once again, the sapphire showed absolutely no indication of optical change at any pump power.

4.6 Intensity Measurement at Beam Center Using Pin Diode

Yet another idea to detect thermal lensing stemmed from the fact that the Nd:YAG pump laser was Q-switched. This meant that there was not actually a steady stream of light, but short pulses, on the order of nanoseconds, at 1 kHz. It was thought that it could be possible for the heat absorbed by the sapphire to dissipate in the crystal causing a thermal lens to only exist for a very, very short period of time. This seemed possible because of the factor of 36 difference in thermal conductivity between glass ($1.11 \frac{W}{m \cdot K}$) and sapphire ($40 \frac{W}{m \cdot K}$) [6]. In order to detect thermal lensing on a fast time scale, a pin diode was placed at the center of the beam a great distance past the thermal lens detecting only the central portion of the beam. If there was any thermal lensing the beam profile would change, changing the intensity of the light hitting the pin diode.

The pin diode was connected to a digital oscilloscope. The Q-switch output of the Nd:YAG laser was also connected to the oscilloscope as the trigger. The oscilloscope was set to show both the trigger input from the Q-switch of the Nd:YAG pump laser, and the Ti:sapph laser oscillator signal on the pin diode. The oscillator was used instead of the HeNe laser so that we could look at individual pulses going through the medium. When a Nd:YAG pulse and a Ti:sapph oscillator pulse were in the medium at similar times, a change in the intensity of the Ti:sapph signal on the pin diode was expected. The samples, glass and sapphire, were tested using this setup at 20 amps diode pump current.

4.6.1 Intensity Measurement at Beam Center Using Pin Diode Results

When testing glass, we saw the initial intensity level of the oscillator pulses decrease. This corresponds to sampling the beam intensity on the opposite side of the focal point since the beam is diverging. The intensity eventually reached an equilibrium value. This was expected since the heat remains concentrated in one place in the glass and develops a thermal lens. Next, the sapphire was tested. It was expected that a change in intensity would be observed when both oscillator pulses and an Nd:YAG pulse coincided in the medium. Again, this was not the case. There was absolutely no detectable change in the intensity of the oscillator pulses traveling through the sapphire even at a fast time scale.

4.7 Effect of Cooling on Thermal Lensing in Glass

Since the build up of heat is the largest contributor to thermal lensing, it is only obvious to try to remove the heat from the medium. In this experiment we attempted to cool the microscope slide with liquid nitrogen to temperatures well below freezing and see what effects the cooling had on the focal length of the thermal lens.

To cool the microscope slide, we bonded it to the copper crystal holder over the existing hole using cpu thermal paste. With the crystal removed, we had a small opening with which to shoot the lasers while keeping most of the slide in contact with the crystal mount. The mount was connected to a liquid nitrogen dewer and mounted in the same configuration as the focal length measurement experiment. A thermocouple was also installed on the crystal mount so that the temperature could be monitored. The pump power was turned up to 20 amps diode pump power and the liquid nitrogen turned on.

It was expected that condensation would form on the crystal mount and microscope slide since it was not housed in an evacuated chamber. With the intense heat of the laser we were confident that the condensation would not form on the parts of the slide where the lasers passed. This seemed to be the case, but the beam was interrupted in another way. A jet of fog about 8 inches long shot out the back side of the crystal mount at a rather high speed from the crystal mounting hole. There was enough fog to block the red probe beam making measurements impossible.

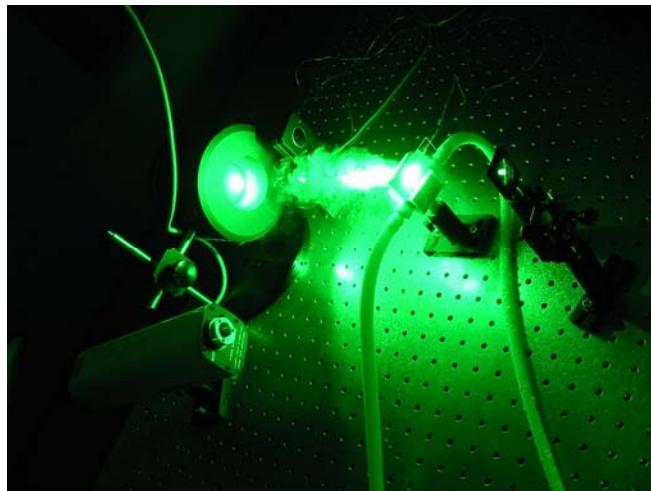


Figure 25: This figure shows the jet of fog being shot out the back of the crystal mount under pump power.

5 Conclusions and Future Work

5.1 Conclusions

It was rather disappointing that thermal lensing was never observed in the sapphire crystal, but the reasons why can be explained. The sapphire crystal was meant to simulate the doped lasing crystal Ti:sapph. Inherently, lasing media have high absorption in order to achieve population inversion. This absorption of light contributes

to the heat deposited in the crystal. Without the doped Ti:sapph, we did not have the high absorption. Combining this with the high thermal conductivity of the sapphire, we simply could not get enough heat to build up in the crystal to cause any detectable optical change. The lack of data from the sapphire also prevented us from testing the accuracy of equation (3-2) for cylindrical optics with fixed temperature boundary conditions.

On a positive note, glass showed thermal lensing very well. In every case we were able to see the effects of thermal lensing in one form or another. The imagery techniques which were developed were also very pleasing, and proved to be very sensitive to optical change, showing the effects in glass very well. The measured values for focal length for varying absorbed pump power proved to follow our expectations of inverse proportionality as seen in the model for a cylindrical optic.

5.2 Future Work

The next stage of research would be to examine the effects of cooling on focal length in a proper evacuated chamber. Understanding this relation could prove an effective way of reducing or even getting rid of thermal lensing in laser amplifiers. An examination of Ti:sapph itself should also be conducted, since it has different characteristics than the sapphire crystal used in this experiment. The higher absorption of the material would in all likelihood make it more conducive to heat build-up and observation of thermal lensing.

References

- [1] Griffiths, David J. Introduction to Electrodynamics 3rd Ed. Prentice Hall. Upper Saddle River, New Jersey: 1999.
- [2] Llewellyn, Ralph A.; Tipler, Paul A. Modern Physics 3rd Ed. W. H. Freeman and Company, New York: 2000.
- [3] Silfvast, William T. Laser Fundamentals Cambridge University Press. New York, NY, 1996.
- [4] Backus, S.; Durfee III, C.G; Murnan, M. M.; Kapteyn H. C. ‘High Power Ultrafast Lasers,’ *Review of Scientific Instruments*, volume 69, number 3.
- [5] Koechner, W.; Bass, M. Solid-State Lasers. Springer. New York, NY. 2003.
- [6] Harrington, J. A. “Infrared Fiber Optics.”
http://irfibers.rutgers.edu/pdf_files/ir_fiber_review.pdf.
- [7] Petersilka, M. and Gross, E. K. U., “Strong-Field Double Ionization of Helium: A Density-Function Perspective,” *Laser Physics*, volume 9, number , 1999.